Rev.Adv.Mater.Sci. 25 (2010) 107-112

MICROSTRUCTURE EVOLUTION IN A CAST 1421Al ALLOY DURING HOT EQUAL-CHANNEL ANGULAR EXTRUSION

F. Musin[1], A. Belyakov[2], R. Kaibyshev[2], Y. Motohashi[3], G. Itoh[4] and K. Tsuzaki[5]

[1]Ufa State Aviation Technical University, K.Marx str., 12, Ufa, 45000, Russia
[2]Belgorod State University, Pobeda 85, Belgorod 308015, Russia
[3]Research Center for Superplasticity, Ibaraki University, Nakanarusawa-cho, 4-12-1, Hitachi, Ibaraki, 316-8511, Japan
[4]Department of Mechanical Engineering, Ibaraki University, Nakanarusawa-cho, 4-12-1, Hitachi, Ibaraki, 316-8511, Japan
[5]Structural Metals Center, National Institute for Materials Science, Sengen 1-2-1, Tsukuba, Ibaraki 305-0047, Japan

Received: December 15, 2009

Abstract. Microstructure evolution during equal channel angular extrusion at 400 °C was studied in a cast 1421Al alloy. The structural changes were investigated by using transmission and scanning electron microscopes incorporating an orientation imaging microscopy. The microstructure evolution is characterized by the development of new fine grains with a size of about 2 μm primarily at triple junctions and near original grain boundaries, leading to the formation of necklace-like microstructure. The interlayers consisting of new fine grains do enlarge with increasing the total strain that results in a gradual rise of the volume fraction occupied by fine grains. The mechanism for the fine-grained microstructure evolution is discussed as a kind of continuous dynamic recrystallization.

1. INTRODUCTION

In the past decade, considerable interest has been aroused among materials scientists and metallurgical engineers in production of ultra fine-grained aluminum alloys by intense plastic straining. Equal channel angular extrusion (ECAE) was considered as an attractive techniques for development of ultra fine grains in relatively large billets of aluminium alloys [1-10]. Cold to warm working by ECAE was shown to result in the formation of submicrocrystalline structures in numerous aluminium alloys [3-10]. Despite of much activity in this field, only a limited number of studies was focused on the mechanism of grain refinement during severe deformation [2,4-7,9]. At low temperatures, the new nanoscale grains developed as a result of grain subdivision mechanism, i.e. formation of dislocation subboundaries like dense dislocation walls followed by a gradual increase in their misorientations that finally led to the development of new fine-grained microstructures. In the previous study [11], the new grain development in an Al-Li-Mg-Sc alloy during ECAP at moderate temperature of 300 °C was dis-

Corresponding author: F. Musin, e-mail: f-musin@ya.ru

cussed in terms of continuous dynamic recrystallization, which has been originally proposed for hot working by conventional deformation methods [12-16]. Generally, the new grain development via continuous dynamic recrystallization (CDRX) involves three elementary mechanisms: (i) formation of arrays of low-angle subboundaries; (ii) transformation of the subboundaries into high-angle boundaries due to accumulation of mobile dislocations; (iii) the elimination of lattice dislocations and subboundaries, leading to a steady state deformation behaviour. However, the microstructure evolution during ECAE at elevated temperatures has not been studied in sufficient detail. The structural mechanisms responsible for the development of new high-angle grain boundaries are still unclear.

The aim of the present work is to study the microstructure evolution in a cast Al-Mg-Li-Sc alloy during ECAE at 400 °C. This study is focused on the structural mechanisms leading to the formation of new fine grains during large strain deformation.

2. EXPERIMENTAL

A 1421 aluminum alloy with a chemical composition of Al-4.1%Mg-2%Li-0.16%Sc-0.07%Zr (in weight pct.) was manufactured by direct chill casting and then was solution treated at 460 °C for 12 hours. The ingot was machined into rods with a diameter of 20 mm and a length of 100 mm. The samples were deformed by ECAE using an isothermal die, circular in cross-section, containing L-type intersecting channels with 90° bend. Extrusion through this die resulted in a strain of about 1 at each pass [2,6]. The samples were extruded to several strains (namely: 1, 2, 4, 8, and 12 passes) at 400 °C. Route A, in which the specimen is repetitively extruded in the same sense without any rotation, was used [2,4,6]. The ram speed was about 2 mm/s. The repetitive extrusion was continuously conducted without any intermediate holdings in a separate furnace. Total time, at which the specimen was held at deformation temperature during ECAE processing and reloading, was ~2 min per each extrusion pass. The deformed specimens were water quenched after the final extrusion pass. To study the static annealing effect on the deformation microstructures, some extruded samples were annealed in a muffle furnace for 2 hours at 400 °C.

Structural analysis of the deformed samples was carried out on sections parallel to longitudinal direction of the extruded rods. The deformation microstructures were studied by various metallographic methods: optical microscopy (OM), scanning electron microscopy incorporating an orientation imaging system (OIM), and transmission electron microscopy (TEM). At least ten typical areas in each sample were analyzed to estimate the evolved grain sizes and the recrystallized volume fractions. The OM/TEM (sub)grain sizes were measured by the linear intercept method and the recrystallized fraction was evaluated by the point-count technique. Strain-induced misorientations between (sub)grains were studied by electron backscatter diffraction technique with OIM software provided by TexSem Lab., Inc. Depending on magnification, various step sizes between analyzed points were set up for OIM micrographs. The step size in each OIM picture can be evaluated by division of the scale mark by the number of steps that are indicated on figures. An average Confidence Index for the indexing of the OIM maps was about 0.7. Low and high angle boundaries were conventionally defined as being less, or greater, than 15°, respectively. For TEM examinations, the samples were thinned to about 0.2 mm and then electro-polished to perforation with Tenupol-2 twinjet polishing unit using 70%CH_3COOH + 30%HNO_3 solution at –20 °C and 6 V. The electron diffraction patterns were obtained from the selected areas of 10 μm in diameter.

3. RESULTS

The initial microstructure after solution treatment consisted of coarse equiaxed grains with an average size of ~60 μm. Two kinds of second-phase particles were identified by the TEM: the Al_2LiMg with a size ranging from 0.5 to 1.0 μm and the Al_3(Sc, Zr) dispersoids with a size of 20 to 60 nm. Interparticle spacing between the Al_3(Sc, Zr) dispersoids was about 300 nm [11].

Typical deformation microstructures are shown in Fig. 1. These microstructures are represented by OIM maps, where the low-angle subboundaries (misorientations from 2 to 15 degrees) and the high-angle grain boundaries (misorientations above 15 degrees) are indicated by thin and thick lines, respectively. It is seen that one ECAE pass leads to the appreciable elongation of initial grains along the extrusion axis as well as the evolution of many subboundaries (Fig. 1a). It should be noted that the subboundary densities are higher in the vicinity of initial grain boundaries than those in the grain interiors. This suggests the large local strain gradients near grain boundaries. The formation of new equiaxed fine grains appears mainly near the triple junctions of initial grain boundaries (Fig. 1b). The

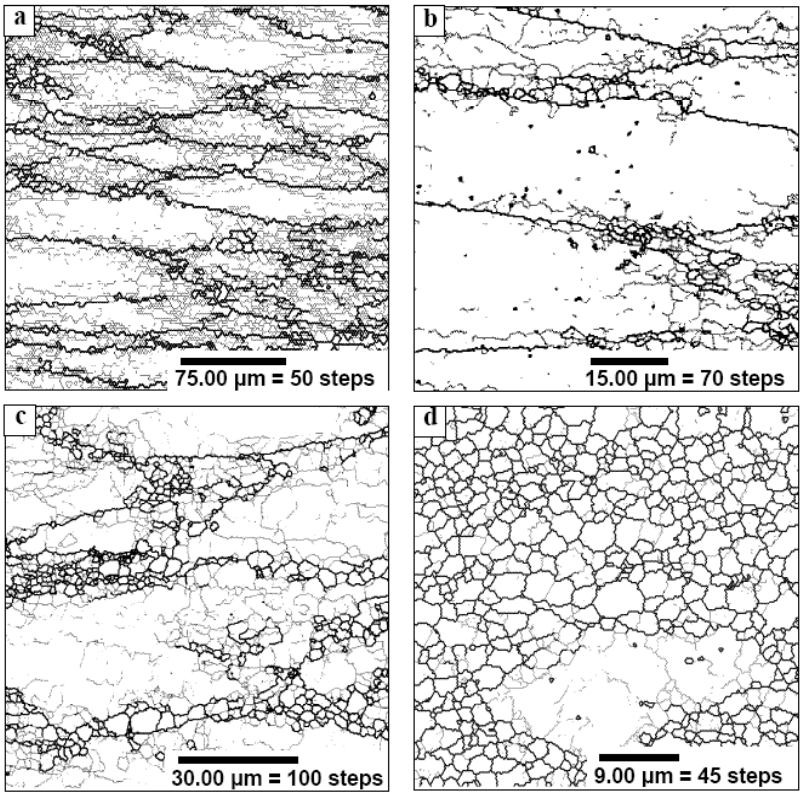

Fig. 1. Typical OIM microstructures evolved in a 1421 alloy processed by ECAE at 400 °C; (a,b) one ECAE pass, (c) two passes, and (d) eight passes. Thin and thick lines correspond to low-angle (>2°) and high-angle (>15°) boundaries, respectively. Note that the extrusion axis is horizontal.

size of these grains is about 2 μm and their volume fraction is ~6%.

The second pass leads to the evolution of a number of new fine grains along the initial grain boundaries (Fig. 1c) making up a necklace surrounding the initial grains. The volume fractions of the recrystallized grains increase with strain and amount to ~30% and ~80% after 4 and 8 passes, respectively. Upon further ECAE processing, the fine new grains propagates into unrecrystallized interiors of initial grains, finally resulting in almost full development of the ultrafine grained microstructure (Fig. 1d).

Typical TEM micrographs for deformation (sub)structures are shown in Fig. 2. The first ECAE pass results in the formation of well-defined subgrain structure throughout the initial grain interiors (Fig. 2a). The subgrain size is about 2 μm. The selected area diffraction pattern forms a net with well-defined diffraction spots, indicating the low-angle misorientations between subgrains. (Sub)grain size revealed by TEM remains apparently unchanged with increasing strain. However, the ring-like diffraction pattern with many scattered diffraction spots in Fig. 2b suggests the rather high-angle misorientations for (sub)grain boundaries evolved after 8 passes. Thus, the OIM and TEM investigations show that the subgrains evolved at early stages of deformation are replaced by the fine grains with high-angle boundaries at high strains.

The average (sub)grain size revealed by various techniques and the volume fraction of new fine grains in 1421 alloy processed by ECAE are presented in Table 1. It is clearly seen that the average subgrain size of 2 μm evolved at early deformation is almost unchanged with further straining. Note here, the (sub)grain sizes determined by three different techniques are almost the same. It should be noted that the static annealing at 400 °C for two hours does not lead to remarkable changes of the ECAE processed microstructures (Table 1). These data suggest that the new grains during hot ECAE of the 1421 Al are indeed formed via dynamic recrystallization. Referring to almost the same (sub)grain sizes, such a process of microstructure evolution

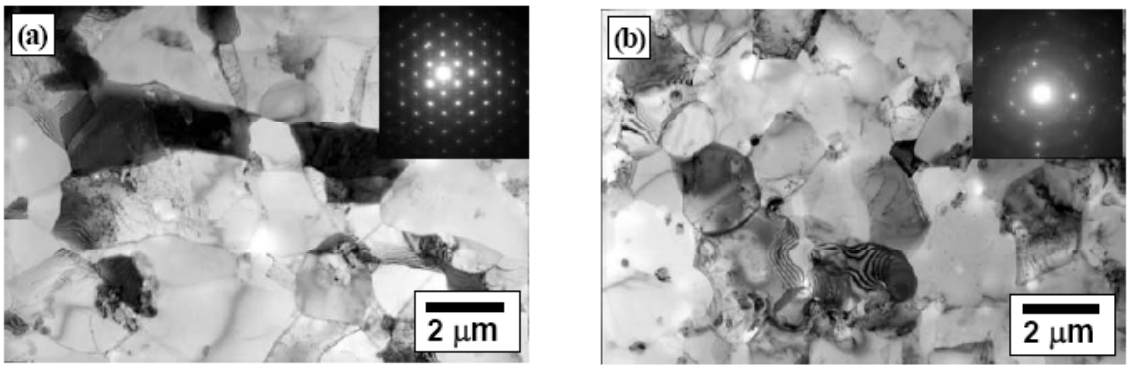

Fig. 2. Typical TEM micrographs of the ECAE substructures evolved in a 1421 alloy; (a) one pass and (b) eight passes. The electron diffraction patterns were obtained from the selected areas of 10 μm in diameter.

can be considered as continuous dynamic recrystallization [13-15].

Fig. 3 shows the volume fraction of recrystallized grains, the area fraction of high angle grain boundaries (HABs) and the average (sub)grain boundary misorientation *vs* the cumulative strain. It is seen that the volume fraction of recrystallized grains and the area fraction of HABs gradually increase with strain, approaching an apparent saturation of about 80% at cumulative strains of above 8. The similar behaviour shows the average (sub)boundary misorientation, namely it increases from about 10 to 30 degrees with straining from one to eight ECAE passes. It is interesting to note for cumulative strains of below 8 that the fraction of recrystallized grains can be represented by a linear function of strain. Extrapolation of this line to zero recrystallized fraction gives a strain of about 0.4. By analogy with a conventional (discontinuous) dynamic recrystallization [13], this strain can be considered as a critical one, which is required for an initiation of recrystallization during ECAE under present conditions.

4. DISCUSSION

The present results suggest that the structural changes in the 1421 alloy during ECAE at 400 °C are associated with continuous dynamic recrystallization, i.e. the new grains with high-angle boundaries are formed by the progressive rotations of subgrains [13]. Arrays of low-angle boundaries evolve within the initial grain interiors at early deformation. Further straining results in gradual increase in the misorientation of deformation-induced subgrain boundaries, leading to the development of a new fine-grained structure at large strains. The general condition for the CDRX mechanism is the accumulation of geometrically necessary dislocations and subboundaries [13,17,18]. In the 1421 alloy, the coherent $Al_3(Sc,Zr)$ dispersoids play an important role as an effective pinning agent. These particles are very efficient in diminishing the effect of static annealing [12] and, therefore, provide the dislocation accumulation within subboundaries during interrupted hot working, i.e. hot ECAE. As a result, (sub)grain size is almost unchanged with increasing strain and an extensive increase in the misorientations between subgrains occurs.

Table 1. The (sub)grain size (*d*) revealed by TEM, OIM, and OM (in the latter case only new fine grains were counted), and the volume fraction of new fine grains (*V*) in 1421 alloy processed by ECAE at 400 °C. Data for the samples annealed at 400 °C for 2 h after 2 and 4 ECAE passes are also included in round brackets.

Number of ECAE passes	1	2	4	8	12
d, μm, by TEM	2.0	2.0	1.9	1.7	1.7
d, μm, by OIM	3.8	2.9	2.3	1.7	1.6
d, μm, by OM	2.8	2.6 (2.8)	2.7 (2.9)	-	2.6
V, %	6	12 (12)	30 (32)	80	83

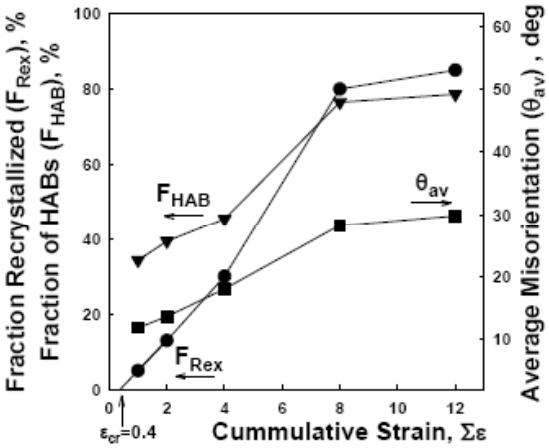

Fig. 3. The volume fraction of recrystallized grains, the area fraction of high angle grain boundaries (HABs) and the average (sub)grain boundary misorientation vs the cumulative strain.

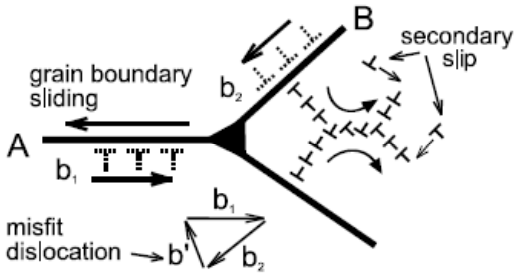

Fig. 4. Long-range misfit stresses caused by grain boundary sliding that evolved near a triple junction of grain boundaries.

The formation of new high-angle grain boundaries rapidly takes place near the original grain boundaries. This may result from the increasing misorientations of geometrically necessary subboundaries, which evolve frequently near the grain boundaries to accommodate strain gradients and long-range internal stresses [19,20]. The latter can be caused by strain incompatibilities associated with grain boundary sliding along initial boundaries. A simple example for the evolution of internal stresses at grain boundary junctions is shown in Fig. 4. The sliding or shearing along boundaries indicated by *A* and *B* necessarily leads to a generation of misfit dislocations at the boundary junction because of geometrical differences in Burgers vectors operating at different boundaries. The accumulation of these misfit dislocations induces high local elastic distortion, which can be released by an initiation of secondary slip. Since the dislocation sources are abundant in grain boundaries, the closely spaced grain boundaries are favourable sites for the secondary multiple slip and, therefore, for the rapid evolution of subboundaries with increasing misorientations. As a result, the recrystallized grains mainly appear at the triple junctions of initial grain boundaries and then along the grain boundaries at relatively small strains of ~1.

A sequence of structural changes associated with CDRX during ECAE of the 1421 Al at 400 °C can be illustrated by a schematic drawing shown in Fig. 5. The first ECAE pass results in the elongation of initial coarse grains along the extrusion axis and the evolution of well-developed subgrains with size of about 2 μm. Dynamic recrystallization may occur even during the first ECAE pass, when the de-

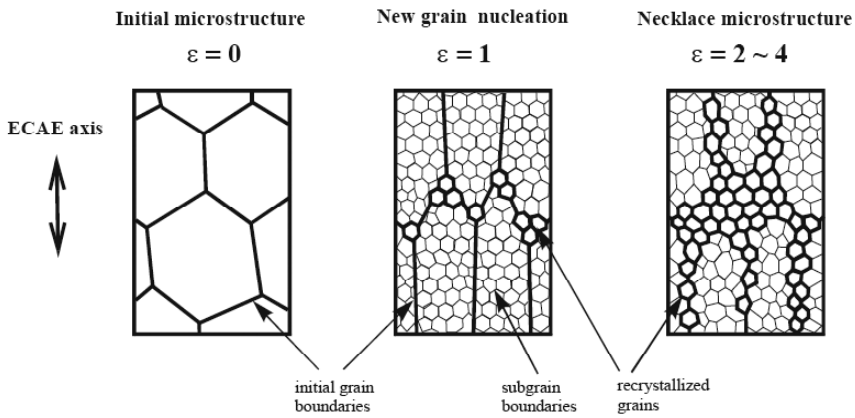

Fig. 5. Schematic drawing of the structural changes taking place in a 1421 alloy during hot ECAE.

formation exceeds some critical strain. The new fine grains are readily formed near the junction of initial grain boundaries. Then, the dynamic recrystallization propagates along the initial grain boundaries, leading to the formation of necklace microstructure at intermediate strains of about 2-4. Upon further straining, the recrystallized layers expand and the fraction recrystallized increases up to about 80% at large strains. Apparent inhibition of the recrystallization kinetics at large strains may result from increasing activity of the grain boundary sliding among the fine recrystallized grains. Since, the grain boundary sliding is extensively operative deformation mechanism in this material at 400 °C [10], the plastic flow can localize within the recrystallized layers. As a result, an effective strain in unrecrystallized volumes diminishes, delaying the further recrystallization progress. Finally, it may be interesting to note that the present CDRX behaviour looks similar to that for conventional (discontinuous) dynamic recrystallization taking place during hot working of materials with low-to-moderate stacking fault energy [13,16], although their structural mechanisms are different.

5. CONCLUSIONS

Microstructure evolution in an aluminum alloy of Al-Mg-Li system (1421 alloy) has been studied during equal channel angular extrusion up to 12 passes at 400 °C. The main results can be summarized as follows:

1. The ECAE results in a considerable grain refinement. The new fine-grained microstructure with a grain size of about 2 μm develops at large cumulative strains of above 8.
2. The new fine grains result from continuous dynamic recrystallization. Early deformation brings about the formation of dislocation subboundaries, leading to the evolution of homogeneous substructure with a subgrain size of about 2 μm; misorientations between the subgrains gradually increase with strain, finally resulting in the transformation of the subgrains into the new fine grains with almost the same size of 2 μm.
3. The recrystallized grains primarily develop near the initial grain boundaries and, especially, near the triple junctions. This results in the evolution of necklace-like microstructure at moderate strains. Upon further straining, the fraction recrystallized increases due to expansion of the recrystallized regions into the initial grain interiors.

ACKNOWLEDGEMENT

The financial support by the Russian Foundation for Basic Research under Project no. 08-08-00894 are gratefully acknowledged.

REFERENCES

[1] V.M. Segal // *Mater Sci Eng. A* **197** (1995) 157.
[2] Y. Iwahashi, Z. Horita, M. Nemoto and T.G. Langdon // *Acta Mater.* **45** (1997) 4733.
[3] S. Lee, P.B. Berbon, M. Furukawa, Z. Horita, M. Nemoto, N.K. Tsenev, R.Z. Valiev and T.G. Langdon // *Mater Sci Eng. A* **272** (1999) 63.
[4] A. Golinia, P.B. Prangnell and M.V. Markushev // *Acta Mater.* **48** (2000) 1115.
[5] Y. Iwahashi, Z. Horita, M. Nemoto and T.G. Langdon // *Acta Mater.* **46** (1998) 3317.
[6] S.D. Terhune, D.L. Swisher, K. Oh-Ishi, Z. Horita, T.G. Langdon and T.R. McNelley // *Metall Trans.* **33A** (2002) 2173.
[7] A. Belyakov, T. Sakai, H. Miura and K. Tsuzaki // *Phil Mag. A* **81** (2001) 2629.
[8] Z.C. Wang and P.B. Prangnell // *Mater Sci Eng. A* **328** (2002) 87.
[9] J.R. Bowen, P.B. Prangnell and F.J. Humphreys // *Mater Sci Techn.* **16** (2000) 1246.
[10] F. Musin, R. Kaibyshev, Y. Motohashi, T. Sakuma and G. Itoh // *Mater Trans JIM.* **43** (2002) 2370.
[11] R. Kaibyshev, K. Shipilova, F. Musin and Y. Motohashi // *Mat. Sci. Eng. A* **396** (2005) 341.
[12] T.G. Nieh, L.M. Hsiung, J. Wadsworth and R. Kaibyshev // *Acta Mater.* **46** (1998) 2789.
[13] F.J. Humphreys and M. Hatherley, *Recrystallization and related annealing phenomena* (Pergamon Press, Oxford, 1996).
[14] S. Gourdet and F. Montheillet // *Mater Sci Eng. A* **283** (2000) 274.
[15] A. Gholinia, F.J. Humphreys and P.B. Prangnell // *Mater Sci Techn.* **16** (2000) 1251.
[16] T. Sakai, J.J. Jonas, In: *Encyclopedia of materials: science and technology,* ed. by K.H. Buschow *et al*. (Elsevier: Oxford, 2001), vol. 7, p. 7079.
[17] K. Tsuzaki, X. Huang and T. Maki // *Acta Mater.* **44** (1996) 4491.
[18] F.J. Humphreys, P.B. Prangnell, J.R. Bowen, A. Gholinia and C. Harris // *Phil Trans R Soc Lond A.* **357** (1999) 1663.
[19] D. Kuhlmann-Wilsdorf and N. Hansen // *Scripta Metall Mater* **25** (1991) 1557.
[20] A. Belyakov, W. Gao, H. Miura and T. Sakai // *Metall Mater Trans A.* **29A** (1998) 2957.